

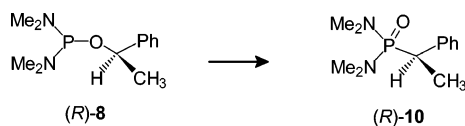
Effect of Amino Substituents on the Stereochemical Outcome of the Photo-Arbuzov Rearrangements of 1-Arylethyl Phosphorodiamidites

Worawan Bhanthumnavin[†] and Wesley G. Bentrude*

Department of Chemistry, University of Utah, Salt Lake City, Utah 84112

bentrude@chem.utah.edu

Received December 31, 2004

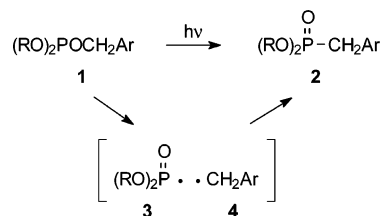


The essentially stereochemically pure 1-arylethyl phosphorodiamidites **8** and **9** were irradiated by UV light in acetonitrile, benzene, and cyclohexane (Tables 1–4). Reaction via *singlet* free-radical pairs, formed by carbon–oxygen bond scission (Scheme 1), which are somewhat longer lived than those from the analogous phosphites **5** and **6**, is proposed. Tetramethyl 1-phenylethylphosphorodiamidite (**8**) gives the photo-Arbuzov rearrangement product **10** in $59\% \pm 2\%$ GC yield, based on percent **8** consumed (Tables 1 and 4), along with the free radical dimerization product 2,3-diphenylbutane, **12a**, in amounts corresponding to ca. 19% of the potentially formed 1-phenylethyl radicals. Similarly, from **9**, the photorearrangement product **11** is generated in $64 \pm 4\%$ yield (Tables 2 and 4) along with a $18 \pm 2\%$ accountability of the 1-naphthylethyl radicals as **12b**. The photorearrangement of stereochemically enriched **8** ($R/S = 99:1$) gives **10** in which an *apparent* $67 \pm 2\%$ (100y, eq 3, Table 4) of the initial radical pairs [**3,14**] recombine with retention of configuration at the stereogenic carbon ($34 \pm 3\%$ net retention, eq 5). With TEMPO present, 70% (100y, eq 3) of the initial 1-phenylethyl radicals, **14**, from **8** combine with radicals **3** in the solvent cage with retained configuration at carbon (40% percent net retention, eq 5). The yield of product **10** is reduced to 54%, and **12a** is absent. Similarly, the five-membered ring naphthylethyl analogue, phosphorodiamidite **9** ($R/S = 98:2$), affords largely (*R*)-**11** with apparent $34 \pm 3\%$ net retention. The degree of stereorandomization observed in these systems is *higher* than was reported previously for phosphites **5** and **6**. The neglect of reconversion of *pro-S* **14** to *pro-R* **14** on the results of these studies is addressed. Estimated *maximum* values (eq 4) of $k_{\text{comb}}/k_{\text{rot}}$ (2.3) for the proximate radical pairs [**3,14**] from **8** with TEMPO present appear to be at least 6-fold *smaller* than those of the analogous phosphite (*R*)-**5** (average $k_{\text{comb}}/k_{\text{rot}} = 13$ with TEMPO present). Possible origins for this effect are proposed.

Introduction

The photo-Arbuzov rearrangements of arylmethyl phosphites **1** to the phosphonates **2** upon direct irradiation with UV light, reported by this laboratory,^{1–3} have been shown to be synthetically useful.^{4,5} Product,³ ³¹P CIDNP,⁶ and CIDEP⁷ (chemically induced dynamic electron po-

larization) studies of **1** (Ar = Ph, *p*-MeCOC₆H₅, 1-naphthyl) are reasonably interpreted in terms of radical pair intermediates [**3,4**]. In our recent report on the photolysis



of optically active phosphites, it was demonstrated that the predominantly singlet or triplet nature of the radical pair can be controlled by phosphite structure or use of triplet sensitizers.⁸ In addition, the observed stereochem-

[†] Present address: Department of Chemistry, Faculty of Science, Chulalongkorn University, Phyathai Rd., Patumwan, Bangkok 10330, Thailand.

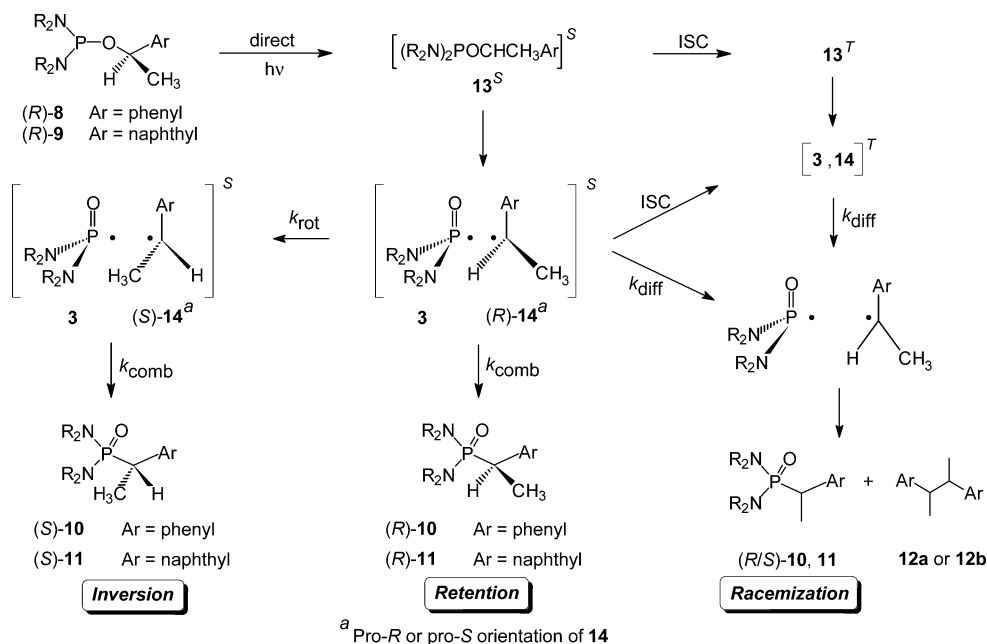
(1) Omelanzuk, J.; Sopchik, A. E.; Lee, S.-G.; Akutagawa, K.; Cairns, S. M.; Bentrude, W. G. *J. Am. Chem. Soc.* **1988**, *110*, 6908–6909.

(2) Cairns, S. M.; Bentrude, W. G. *Tetrahedron Lett.* **1989**, *30*, 1025–1028.

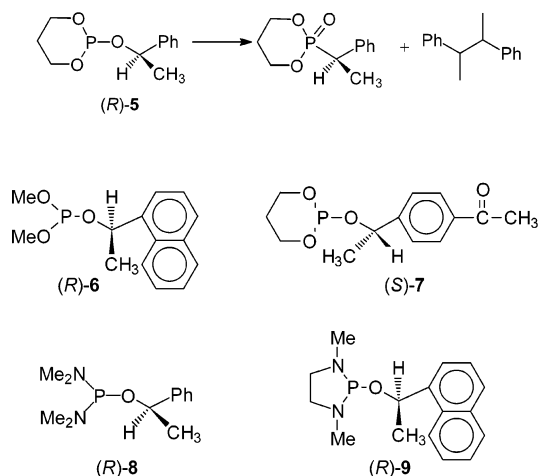
(3) Ganapathy, S.; Soma Sekhar, B. B. V.; Cairns, S. M.; Akutagawa, K.; Bentrude, W. G. *J. Am. Chem. Soc.* **1999**, *121*, 2085–2096.

(4) Bentrude, W. G.; Mullah, K. B. *J. Org. Chem.* **1991**, *56*, 7218–7224.

SCHEME 1



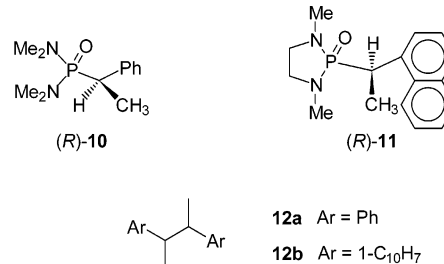
istry at the migratory carbon of stereochemically enriched, chiral phosphites was correlated with the multiplicity of the radical pair generated. Presumed proximate



singlet radical pairs $[3,14]^S$, analogous to those of Scheme 1, generated from direct irradiation of phosphites **5** and **6**, give products with a high degree of retention of configuration (80% net retention for **5** with TEMPO present and 86% net retention for **6** without TEMPO). By contrast, triplet radical pairs, produced from direct irradiation of **7** or triplet sensitized photolysis of **6**, yield essentially racemic products.⁸

We report here the effect of changing the substituents on phosphorus on the product distribution and stereo-

chemical outcome. The photolysis of nearly stereochemically pure (*R*)-1-phenylethyl *N,N,N',N'*-tetramethylphosphorodiamidite ((*R*)-**8**) and the 1-naphthylethyl analogue, 2-(1-naphthylethoxy)-1,3-dimethyl-1,3,2-diazaphospholane ((*R*)-**9**), both of which have two amino substituents on phosphorus, to give products **10** and **11** was carried out. The stereochemical outcome and product yields



involving the presumed initial caged radical pair from **8** ($[3,14]^S$, Scheme 1) were determined in the presence of the free-radical scavenger 2,2,6,6-tetramethylpiperidin-1-oxyl (TEMPO). The extent of retention of configuration at the stereogenic carbon was determined, and estimates of the relative rate constants for cage combination (k_{comb}) and rotation (k_{rot}) were made. These systems are highly suitable for measurement of the competition between cage combination and rotation because we are able to show that the starting phosphorodiamidites, (*R*)-**8** and (*R*)-**9**, and the products **10** and **11** are stereochemically stable under the photoreaction conditions. Errors that result from not considering the reversibility of the conversion of pro-*R* **14** to pro-*S* **14** (Scheme 1) are addressed in detail.

Results

Preparation of 8 and 9. Isolation of Photorearranged Products. Determination of Enantiopurity. Phosphorodiamidites **8** and **9** were prepared from the requisite phosphorus triamide and either the racemic

(5) Mullah, K. B.; Bentrude, W. G. *Nucleosides Nucleotides* **1994**, *13*, 127–153.

(6) Koptuyug, I. V.; Sluggett, G. W.; Ghatlia, N. D.; Landis, M. S.; Turro, N. J.; Ganapathy, S.; Bentrude, W. G. *J. Phys. Chem.* **1996**, *100*, 14581–14583.

(7) Koptuyug, I. V.; Ghatlia, N. D.; Sluggett, G. W.; Turro, N. J.; Ganapathy, S.; Bentrude, W. G. *J. Am. Chem. Soc.* **1995**, *117*, 9486–9491.

(8) Bhanthumnavin, W.; Bentrude, W. G. *J. Org. Chem.* **2001**, *66*, 980–990.

TABLE 1. Yields and Stereochemical Results for the Photorearrangement of 8 (*R/S* = 99:1)^a

solvent	conversion of 8 ^b (%)	accountability yield ^b (%)		<i>R/S</i> ratio of 10 ^{d,e}
		10	12a ^c	
acetonitrile	16	57	18	67:33
acetonitrile	25	59	20	65:35
acetonitrile	100	60	20	66:34
cyclohexane	19	62	20	67:33
cyclohexane	27	59	18	69:31
cyclohexane	95	61	20	66:34
benzene	18	56	18	67:33
benzene	29	57	16	68:32

^a Ca. 0.01 M **8** at 254 nm, 35–40 °C. ^b By GC analysis. Based on the amount of consumed **8**. ^c Yield of **12a** doubled to account for the stoichiometry of its formation from **8**. ^d Determined by chiral HPLC on a CHIRALCEL OD column. ^e Average 67/33.

TABLE 2. Product Yields and Stereochemical Results Obtained from Direct Irradiation of 9 (*R/S* = 98:2)^a

solvent	conversion of 9 ^b (%)	accountability yield ^b (%)		<i>R/S</i> ratio of 11 ^{d,e}
		11	12b ^c	
acetonitrile	24	68	18	63:37
acetonitrile	43	59	16	69:31
acetonitrile	97	60	18	67:33
cyclohexane	18	65	20	70:30
cyclohexane	40	68	18	65:35
cyclohexane	100	67	18	67:33

^a Ca. 0.01 M **9** at 300 nm, 35–40 °C. ^b By GC analysis. Based on the amount of consumed **9**. ^c Yield of **12b** doubled to account for the stoichiometry of its formation from **9**. ^d Determined by chiral HPLC on a CHIRALCEL OD column. ^e Average 67/33.

alcohol or stereoisomer of *R* configuration and high enantiomeric purity (97–98% ee). Photolysis of racemic **8** and **9** yielded the photorearranged products **10** and **11**, isolated by HPLC, and the radical dimer **12**. The initial enantiopurities of very largely *R*-form **8** and **9** were determined, following their retentive conversion⁹ by *t*-BuOOH to their oxides, HPLC purification, and chiral HPLC analysis (baseline-resolved) on a CHIRALCEL OD column as described in detail earlier for the phosphates from oxidation of **5** and **6**.⁸ The *R/S* ratios were the same as those of the starting alcohols. Unreacted stereochemically enriched **8** and **9** were similarly oxidized and analyzed by chiral HPLC at various photochemical conversions as were the products **10** and **11**. The *R/S* ratios of the oxides remained unchanged (see the Supporting Information.). Therefore, if the caged radical pairs [**3,14**] recombine, they do so with retention of configuration at carbon. As a result, any loss of configuration arises during formation of **10** or **11**.

Products **10** and **11** from optically enriched **8** or **9** were purified by HPLC, and the enantiomeric ratios (Tables 1–3) were determined on a CHIRALCEL OD HPLC column as described previously⁸ for the stereochemically enriched phosphonates from **5** and **6**. The predominant enantiomer of **10** and **11** was assigned the *R* configuration based on the known retentive stereochemistry of the photo-Arbuzov rearrangement of phosphites determined by X-ray crystallography and NMR spectroscopy.^{1,10} Product yields (Tables 1–3) were obtained by standard quantitative GC measurements.

(9) Bentrude, W. G.; Hargis, J. H. *J. Am. Chem. Soc.* **1970**, *92*, 7136–7144.

TABLE 3. Photolysis of 8 (*R/S* = 99:1) in the Presence of Radical Trap TEMPO^a

8/TEMPO	conversion of 8 ^b (%)	accountability yield ^b (%)		<i>R/S</i> ratio of 10 ^d
		10	12a ^c	
<i>e</i>	29	62	20	68:32
<i>e</i>	19	59	20	69:31
<i>e</i>	27	61	20	69:31
1:0.8	31	59	16	68:32
1:1.0	21	58	12	69:31
1:1.2	25	56	12	70:30
1:1.5	24	56	10	70:30
1:1.8	29	55	4	71:29
1:2.0	20	54	0	70:30
1:2.5	33	55	0	70:30
1:3.0	19	54	0	71:29

^a Ca. 0.01 M **8**, cyclohexane solvent at 254 nm, 35–40 °C. ^b By GC analysis. Based on the amount of consumed **8**. ^c Yield of **12a** doubled to account for the stoichiometry of its formation from **8**. ^d Determined by chiral HPLC on a CHIRALCEL OD column. ^e No TEMPO added.

Photorearrangement of Stereochemically Enriched Phosphorodiamidite 8 (*R/S* = 99:1). Phosphorodiamidite **8** (ca. 0.01 M) of predominately *R* configuration was irradiated at 254 nm through quartz in acetonitrile, benzene, and cyclohexane solvents. Product yields and stereochemical results are summarized in Table 1. Rearrangement product **10** was formed in 59 ± 2% yields (GC, Tables 1 and 4) along with an average yield of 2,3-diphenylbutane (**12a**, two pairs of enantiomers separable by GC) corresponding to 19 ± 2% of the potentially formed 1-phenylethyl radicals (Tables 1 and 4). Partial racemization was observed in product **10**. Starting with **8** of 99:1 *R/S* ratio, an average (*R/S*) enantiomeric ratio of 67:33 was encountered in product **10** (34 ± 3% percent net retention, eq 5, Table 4). (*R/S* ratios are based on percentages of total product, *R* plus *S*.) The *R/S* ratios of the product **10** (Table 1) and **8** (Supporting Information) are largely constant regardless of the percent conversion of (*R*)-**8**. In a control reaction photoproduct (*R*)-**10** (99% ee) was irradiated under photoreaction conditions. Its enantiopurity remained unchanged. Thus, both **8** and **10** are configurationally stable.

Photorearrangement of Stereochemically Enriched 2-(1-Naphthylethyl)diazaphospholane 9 (*R/S*) = 98:2. Phosphorodiamidite **9**, the five-membered ring 1-naphthylethyl analogue of **8**, was irradiated at 300 nm through Pyrex in acetonitrile and cyclohexane solvents (ca. 0.01 M). Product yields (64 ± 4%) and stereochemical results for **9** are similar to those for phosphorodiamidite **8**. Rearrangement product **11** was formed in 64 ± 4% yield along with (**12b**) corresponding to an 18 ± 2% accountability of 1-naphthylethyl radicals (Tables 2 and 4). Other radical products such as 1-ethylnaphthalene (or ethylbenzene from **8**) were observed by GC in trace amounts (GC and GC/MS) but were not quantified. Starting with a 98:2 *R/S* ratio of **9**, the *R/S* enantiomeric ratios in the rearrangement product **11** (67:33) amount to 34 ± 3% net retention at carbon (Table 4). Essentially constant *R/S* ratios for phosphorodiamidite **9** (Supporting Information) and the product **11** (Table 2) were observed as a function of conversion. A solution of 70:30 (*R/S*) **11**, irradiated at a typical concentration of **9** in the stereochemical studies, over the same period of time, had unchanged *R/S* ratios (chiral HPLC). Furthermore, when

TABLE 4. Summary of Photochemical Results

compd	conditions	accountability yield (%)		cage yield product (%)	100y ^d	% net retention ^e	$k_{\text{comb}}/k_{\text{rot}}^g$
		product	dimer ^a				
8	direct $h\nu$	59 ± 2 ^b	19 ± 2	<i>c</i>	67 ± 2 ^b	34 ± 3(34) ⁱ	2.0
8	with TEMPO	54 ^h	0	54	70 ^h	40 ^h (40)	2.3
9	direct $h\nu$	64 ± 4	18 ± 2	<i>c</i>	68 ± 3	34 ± 3 (36)	2.1
5^f	direct $h\nu$	67 ± 2	4 ^h	<i>c</i>	88 ± 2	72 ± 2 (76)	7.3
5^f	with TEMPO	64 ^h	0	65	93 ^h	80 ^h (86)	13
6^f	direct $h\nu$	65 ± 4	3 ± 1	<i>c</i>	95 ± 2	86 ± 3 (90)	19

^a Yield of dimer doubled to account for the stoichiometry of its formation from starting materials. ^b Average deviation from average. ^c TEMPO not added. Cage yield not applicable. ^d Equations 2 and 3. ^e Equation 5. ^f Data from ref 8. ^g Equation 4. ^h Average deviation < 1. ⁱ Numbers in parentheses are based on 100y values.

either **10** or **11** was subjected to the entire workup procedure, their enantiomeric compositions were unchanged.

Photorearrangement of Stereochemically Enriched 8 in the Presence of Nitroxide Radical Scavenger. The stable radical TEMPO is commonly employed to trap free radicals that escape the initial solvent cage and is applicable to both phosphorus- and carbon-centered radicals. Photoexcited TEMPO can extract hydrogen resulting in depletion of radical scavenger concentration. Therefore, the trapping experiment was done in cyclohexane where this side reaction occurs to a lesser extent than in acetonitrile.¹¹ The concentrations of TEMPO used were below those known to trigger the *anti-scavenging effect* noted by Turro and co-workers.¹² Detailed analysis of other products, formed from reactions with TEMPO, was published earlier,^{3,8} including the product of trapping of radical **3** for phosphite **1** with R = Me, Ar = *p*-acetylphenyl.

Irradiation of phosphorodiamidite (*R*)-**8** (*R/S* = 99:1, ca. 0.01 M) in the presence of *increasing amounts* of TEMPO (0.002–0.030 M) was carried out (Table 3). The first 3 entries in Table 3 without added TEMPO are included for comparison. The yield of **10** decreases from 59 ± 2% and levels off at about 54% when the TEMPO concentration exceeds 0.02 M (Tables 3 and 4). Simultaneously, the yields of dimer **12a** decrease until no dimer is found when 2 equivalents or more of the trap are used. Concurrently, a small increase in retention of configuration in product **10** is observed. The initial 67:33 enantiomeric composition (*R/S*) of **10** becomes constant at 70:30 (40% net retention, Tables 3 and 4), presumably corresponding to **10** formed exclusively from [3,14]^S in the solvent cage.

Discussion

Analysis of Stereochemical Results. It is clear from the lack of effect (Tables 1–3) of change to a polar solvent, acetonitrile, that polar effects including ion-pair formation do not influence these reactions. As noted, Scheme 1 summarizes possible pathways for product formation in the photorearrangements of **8** and **9** by a free-radical pair mechanism. The results obtained previously⁸ from the product and stereochemical studies of the photo-

Arbuzov rearrangements of phosphites **5** and **6** are consistent with the key reaction step being *homolysis* of the ArCHMe–OPX₂ bond to give the radical pair analogous to [3,14]^S. Analogously, photochemical excitation of **8** or **9** is proposed (Scheme 1) to produce a singlet excited state, **13^S**, which undergoes homolytic C–O bond dissociation to the corresponding *singlet* geminate radical pair [3,14]^S. On cage recombination, the initial geminate radical pair [3,14]^S involving *pro-R* **14** yields the rearranged product, (*R*)-**10** or (*R*)-**11**, with *retention* of configuration at the prochiral carbon. Rotation of *pro-R* **14** to give *pro-S* **14** prior to combination with **3** affords **10** and **11** with *inverted* carbon configuration. Singlet geminate radical pairs are typically short-lived and predominantly undergo recombination within the solvent cage. Indeed, with the phosphites a relatively high degree of retention of configuration at stereogenic carbon is seen (Table 4).⁸ Diffusion of the radical pair from the solvent cage leads to dimer **12** and *racemized* **10** or **11**. For phosphites **5** and **6**, only 3–4% of **12** is found. Scheme 1 also provides for intersystem crossing of the initially formed singlet excited starting material, **13^S**, to its triplet excited state to generate triplet radical pairs. The possibility that radical pair [3,14]^S is converted to the more long-lived triplet pair, [3,14]^T, also is depicted. The data from Tables 1–3 are condensed and summarized in Table 4 for ease of comparison, along with the earlier results for phosphites **5** and **6**⁸ to facilitate discussion.

When the reconversion of *pro-S* **14** to *pro-R* **14** and radical pair diffusion are negligible, as for **5** and **6**, the stereochemical results can be readily analyzed in terms of Scheme 1 to provide an estimate of the ratio $k_{\text{comb}}/k_{\text{rot}}$ for the radical pair [3,14]. Let R_{SM} and S_{SM} represent the *percentages of starting phosphorodiamidite* in the *R* and *S* configurations, respectively, and R_{obsd} and S_{obsd} be the *percentages of observed product* in the *R* and *S* configurations. The total yields of **10** and **11** are not 100 percent. However, calculation of R_{obsd} and S_{obsd} based on total **10** or **11** formed is reasonable since the formation of products other than **10** or **11** will not be affected by the *R* or *S* configuration at the stereogenic carbon; i.e., inefficiencies in formation of *R* and *S* products are proportionately the same.

By the approach used previously,⁸ let *y* equal the *fraction of initially formed reaction pairs* [3,14]^S from R_{SM} or S_{SM} that combines *before* rotation with *retention* of configuration at the prochiral center of *pro-R* **14**. Then 1-*y* is the fraction of initial R_{SM} or S_{SM} that yields product with *inverted* configuration after conversion of *pro-R* **14** to *pro-S* **14**. The quantity *y* can be readily obtained.⁸

(10) Bhanthumnavin, W.; Bentrude, W. G.; Arif, A. M. *J. Org. Chem.* **1998**, *63*, 7753–7758.

(11) Johnston, L. J.; Tencer, M.; Scaiano, J. C. *J. Org. Chem.* **1986**, *51*, 2806–2808.

(12) Step, E. N.; Buchachenko, A. L.; Turro, N. J. *J. Am. Chem. Soc.* **1994**, *116*, 5462–5466.

Based on the *R* enantiomer:

$$R_{\text{obsd}} = R_{\text{SM}}y + S_{\text{SM}}(1 - y) \quad (1)$$

and

$$y = (R_{\text{obsd}} - S_{\text{SM}})/(R_{\text{SM}} - S_{\text{SM}}) \quad (2)$$

When S_{SM} is negligible

$$y = R_{\text{obsd}}/R_{\text{SM}} = R_{\text{obsd}}/100 \quad (3)$$

Values for y , based on the *R/S* product ratios of Tables 1–3, are given in Table 4 for phosphorodiamidite **8** and **9** on a percentage basis, $100y$. When the percentage of *S* enantiomer, S_{SM} , is only 1% (as for **8**), eqs 2 and 3 give the same value for y . For **5**, **6**, and **9**, S_{SM} is 2–3%, and eq 2 was used to give a slightly higher number for y (e.g., for 0.93 vs 0.90 for **5** with added TEMPO) which, however, is surely within experimental error of that calculated from eq 3.

The relationship between the rate constant for rotation (k_{rot}) and the rate constant for recombination (k_{comb}) simply corresponds (eq 4) to the fraction (y) of radical pairs initially formed within the initial solvent cage that undergoes recombination with **3** before rotation of *pro-R* **14** divided by the fraction that undergoes recombination after one rotation:

$$k_{\text{comb}}/k_{\text{rot}} = y/(1-y) \quad (4)$$

Percent net retention, also recorded in Table 4, is the mechanism-independent quantity calculated from the average $R_{\text{obsd}}/S_{\text{obsd}}$ ratios of Tables 1–3 via eq 5.

$$\% \text{ net retention} = [(R_{\text{obsd}} - S_{\text{obsd}})/(R_{\text{obsd}} + S_{\text{obsd}})] \times 100 = R_{\text{obsd}} - S_{\text{obsd}} \quad (5)$$

Equation 5 assumes that the starting material is 100% in the *R* configuration. There are very small errors in R_{obsd} and S_{obsd} as 1–3% of S_{SM} is present in each case. In parentheses in Table 4 are the slightly higher percent net retention values based on $100y$ whose calculation via eq 2 accounts for S_{SM} in **5**, **6** and **9**; for example, for **9** this number is (68–32) or 36%.

When the rotation of radical **14** (Scheme 1) is reversible, i.e., conversion of *pro-S* **14** back to *pro-R* **14** competes with k_{comb} to give product of *S* configuration, eqs 1–4 are only approximations, since they are based on the assumption that $k_{\text{comb}} \gg k_{\text{rot}}$ rotation. (The reversible rotation of *pro-R* **14** and the potential for the diffusion of the radical pair [*pro-S* **14,3**] from the solvent cage are not shown in Scheme 1, but their inclusion can be readily visualized.) Obviously, if *pro-R* **14** is regenerated from *pro-S* **14** (k_{rot}) in competition with recombination (k_{comb}), the measured or apparent value of R_{obsd} will be increased. Consequently, the apparent or measured y value in Table 4 is larger than it actually is. As a result, the value of $k_{\text{comb}}/k_{\text{rot}}$ based on eq 4 will increase. In addition the apparent or measured percent net retention (eq 5) also will be increased. Moreover, diffusion of the radical pair [**3,14**] from the solvent cage will have an affect on the stereochemical outcome of the processes depicted in Scheme 1. These effects will be discussed below in more detail.

The assumptions that $k_{\text{comb}} \gg k_{\text{rot}}$ and (k_{comb} and k_{rot}) $\gg k_{\text{diff}}$ apply well to phosphites **5** and **6** (Table 1) studied earlier.⁸ Only a small amount of radical dimer **12** (ca. 4% accountability of potentially formed cage-free **14**) is found, and a high degree of retention at carbon is observed (Table 4). Neither ³¹P CIDNP nor ESR signals can be observed on direct UV irradiation of the achiral, 1-naphthylmethyl analogue of phosphite **6**.¹³ These results are consistent with photo reaction via rather short-lived, singlet radical pairs [**3,14**]. By contrast, in the photorearrangements of **8** and **9** relatively large amounts of dimer **12** are formed, and considerable loss of configuration at the stereogenic carbon of products **10** and **11** (Tables 1–4) is noted. Consequently, for **8** and **9** both radical pair diffusion and reversibility of the conversion of *pro-R* **14** to *pro-S* **14** are significant; and the consequent errors in application of eqs 2–5 must be considered.

Singer and co-workers¹⁴ carried out a steady-state treatment of the thermal rearrangement via singlet radical pairs of optically pure (*S*)-MePhCHN=C=CPh₂. Based on a scheme completely parallel to Scheme 1, but including reversible rotation of **14** and diffusion of the radical pairs analogous to [*pro-R* **14,3**]^S and [*pro-S*, **14,3**]^S, they obtained relative values of k_{rot} , k_{comb} , and k_{diff} . However, this treatment requires accurate measurement of the fraction of radicals (f) that escape the solvent cage, $f = k_{\text{diff}}/(k_{\text{diff}} + k_{\text{comb}})$, which is not available from our data. Nonetheless, the effects of rotation of **14** and radical diffusion on measured or apparent y , $k_{\text{rot}}/k_{\text{comb}}$, and percent net retention can be illustrated semiquantitatively with a simple model.

Model for the Effects of Reversibility of *pro-R* **14 Rotation and Radical Diffusion.** Start with **13** (Scheme 1) that is 100% the *R* enantiomer and gives 100 [**3, pro-R 14**]^S radical pairs. In the simplest case, assume that no radical diffusion occurs, but 40 of the initial 100 *pro-R* **14** are converted to 40 *pro-S* **14** (i.e., actual $k_{\text{comb}}/k_{\text{rot}} = 60:40 = 1.5$) which combine with **3** to afford *S* product ($S_{\text{obsd}} = 40$). The remaining 60 *pro-R* **14** couple with **3** to give *R* product; thus, $R_{\text{obsd}} = 60$; $R_{\text{obsd}}/S_{\text{obsd}} = 60:40$; $100y = 60$ (eq 3); percent net retention = 20% (eq 5).

Then, allow the 40 *pro-S* **14** formed from *pro-R* **14** to be apportioned 60:40 between coupling to afford 24 *S* product and reconversion to 16 *pro-R* **14** (again, $k_{\text{comb}}/k_{\text{rot}} = 1.5$), which is subsequently split 60:40 between 10 *R* product and reformation of 6 *pro-S* **14**. The latter divides 60:40 between coupling to yield 4 *S* product and reversion to 2 *pro-R* **14** which combine with **3** to form 2 *R* product. The combined yield of *R* product (R_{obsd}) is 72% (60 + 10 + 2). S_{obsd} is 28, and $R_{\text{obsd}}/S_{\text{obsd}}$ is 72:28. The actual fraction of initial *pro-R* **14** that couple before rotation, y , is $[(1.5)/(1.0 + 1.5)]$ or 0.6. However, the apparent or measured value of y , calculated from R_{obsd} , is 72:100 or 0.72 (eq 3, $100y = 72$). From eq 4 the apparent $k_{\text{comb}}/k_{\text{rot}}$ is $[0.72/(1 - 0.72)]$ or 2.6 which is (2.6/1.5) or 1.7 times the actual $k_{\text{comb}}/k_{\text{rot}}$. This is a small but significant increase in measured or apparent $k_{\text{comb}}/k_{\text{rot}}$ that results from the reversibility of the conversion of *pro-R* **14** to *pro-S* **14**. As noted above, were the formation

(13) Sluggett, G. W.; Landis, M. S.; Ghatlia, N.; Turro, N. J.; Bhanthumnavin, W. unpublished results.

(14) Lee, K.-W.; Horowitz, N.; Ware, J.; Singer, L. A. *J. Am. Chem. Soc.* **1977**, *99*, 2622–2627.

of initial *pro-S* **14** irreversible, the ratio $R_{\text{obsd}}/S_{\text{obsd}}$ would be 60:40 corresponding to a percent net retention of (60 – 40) or 20, eq 5. For the calculated ratio of enantiomers, $R_{\text{obsd}}/S_{\text{obsd}}$ of 72:28, the measured percent net retention is expected to be (72–28) or 44, a larger percentage than in the absence of rotation of radical **14** from the *pro-S* configuration back to the *pro-R* form. It is clear that the reversible interconversion of *pro-R* **14** and *pro-S* **14** increases both apparent $k_{\text{comb}}/k_{\text{rot}}$ and percent net retention.

Inclusion of diffusion in this model with $k_{\text{comb}}/k_{\text{rot}}$ still 1.5, and k_{diff} accounting for 20% of the initial radical pair, decreases the overall rearrangement product yield, changes R_{obsd} and S_{obsd} , increases y and, therefore, the measured $k_{\text{comb}}/k_{\text{rot}}$. Assume again that 100 *pro-R* [**14**,**3**]^S are generated, but now 20 (20%) undergo diffusion. The other 80 pairs are apportioned according to the assumed ratio $k_{\text{comb}}/k_{\text{rot}} = 1.5$ so that 32 *pro-S* **14** are generated by rotation. The remaining 48 *pro-R* **14** (48% of the initial pairs) combine with radical **3** to give *R* product. The relative rate constants are then $k_{\text{diff}}/k_{\text{rot}}/k_{\text{comb}} = 1:1.6:2.4$. Of the 32 *pro-S* **14** generated, 20% or 6 undergo diffusion, 48% or 15 combine with radical **3** to generate *S* product (15%), and 32% or 10 undergo rotation to reform *R*-**14** ($k_{\text{comb}}/k_{\text{rot}} = 1.5$). The 10 *R*-**14** are then apportioned between diffusion (2), combination with **3** to yield *R* product (5), and reformation of *S*-**14** (3), 2 of which afford *S* product along with diffusion (<1) and regeneration of *pro-R* **14** (1). Consideration of the fractional distribution of products of the one *pro-R* **14** does not refine the results beyond the experimental error in the measurement of *R* and *S* products. Total accountabilities are thus as follows: *R* product, 53% (48 + 5); *S* product, 18% (16 + 2); radical diffusion products 29% (20 + 6 + 2 + 1).

As noted above, since the total yield of *R*- and *S*-product is not 100%, the percentages R_{obsd} and S_{obsd} must be based on total rearrangement product formed. Thus, R_{obsd} is $[53/(53 + 18)] \times 100 = 75$, and S_{obsd} is 25. The apparent value of y (eq 3) is 0.75 ($R_{\text{obsd}}/R_{\text{SM}} = 75/100$) and from eq 4 $k_{\text{comb}}/k_{\text{rot}} = 3.0$, $[0.75/(1 - 0.75)]$. Actual y is still 0.6 with $k_{\text{comb}}/k_{\text{rot}} = 1.5$. The apparent or measured $k_{\text{comb}}/k_{\text{rot}}$ is 2.0 times the actual value (3.0/1.5). On a percent net retention basis, the experimental value is 50% (75 – 25) vs the actual value of 20. It may be surprising that inclusion of 20% diffusion of the pairs [**3**,**14**]^S in Scheme 1 has a relatively small, though not negligible, effect on measured or apparent y and $k_{\text{comb}}/k_{\text{rot}}$ when compared to the actual values.

If one assumes 30% diffusion of each radical pairs [**3**,**14**]^S set formed, the same model shows that the combined yield of *R* and *S* products is reduced to 60% (diffusion total 40%) with $R_{\text{obsd}}/S_{\text{obsd}}$ increased to 78:22. Apparent y is increased to 0.78 and $k_{\text{comb}}/k_{\text{rot}}$ to 3.5. This ratio is 2.3 times (3.5:1.5) the actual number. Percent net retention is 56.

The important conclusion from the above considerations is that the values of y in Table 4 are larger than the actual ones so that the numbers for $k_{\text{comb}}/k_{\text{rot}}$ (Table 4) are also higher. As a result, the experimental values for $k_{\text{comb}}/k_{\text{rot}}$ of Table 4 for **8** and **9** are maximum ones. The ratio $k_{\text{comb}}/k_{\text{rot}}$ is expected to be reasonably accurate for **5** with TEMPO present, because as noted earlier, there is little radical pair diffusion, and the high values of 100y (Table 4) indicate that return of *pro-S* **14** to *pro-R*

14 should be minimal. The importance of these considerations in the still-instructive comparison of the values of $k_{\text{comb}}/k_{\text{rot}}$ for **8** and **9** with those for **5** and **6** will be addressed below.

Photorearrangements of Phosphorodiamidite **8 and **9**. Comparison to **5** and **6**.** In summary, the photoreactions of **8** and **9** give the corresponding rearranged products, **10** and **11**, in fair to good accountability yields (Tables 1–4). Significantly, these photoprocesses are accompanied by the formation of about 9–10% of the corresponding 2,3-diarylbutanes (18–20% of potentially formed radicals **14**) which obviously arise from dimerization of free 1-arylethyl radicals that diffuse from the initial solvent cage.

In addition, the stereochemical results (Tables 1–4) reveal that for **8** and **9** a considerable amount of stereorandomization has occurred. Starting with a 99:1 (*R/S*) ratio enantiomeric mixture of phosphorodiamidite **8** and 98:1 (*R/S*) **9**, only about 34% net retention (eq 5) is observed in products **10** and **11**. This number increases to 40% for **8** when the free radical scavenger TEMPO is present, and the radicals that give dimer **12** are trapped completely. Of the radicals **14** formed, 65–70% combine with **3** with retention of configuration. Very significantly, for **8** and **9** the percent retention of configuration of the stereogenic carbon (34%) is considerably lower than is observed (Table 4) in the direct photolysis of the phosphite analog **5** (80% net retention with TEMPO added) and **6** (86%, no TEMPO). The same is true for the values of 100y with TEMPO present; i.e., 93 for **5** versus only 70 for **8**.

That rotation of geminate, *pro-R* 1-phenylethyl radical, **14**, from **8** (Scheme 1) competes well with combination with its phosphinoyl radical partner, **3**, is confirmed by the ratio $k_{\text{comb}}/k_{\text{rot}}$ (2.3, TEMPO added, Table 4) for the 1-phenylethyl radical from **8** (eqn 4). This is much lower than what is seen for the caged pair from phosphite **5** ($k_{\text{comb}}/k_{\text{rot}} = 13$, TEMPO added, Table 4) or for photolysis of **6** without added TEMPO ($k_{\text{comb}}/k_{\text{rot}} = 19$, Table 4).⁸ These results, along with the relatively high yield of dimers **12a** and **12b** and reduced degree of retention of stereochemistry at carbon with both **8** and **9**, compared to those from direct photolysis of **5** and **6**, indicate that irradiation of **8** and **9** yields comparatively long-lived radical pair intermediates. It seems quite certain that reversal of the conversion of *pro-R* **14** to *pro-S* **14** occurs in the photorearrangements of **8** and **9**.

The possibility that the relatively high degree of stereorandomization seen for **8** and **9** results from random combination of radicals **3** and **14** that have escaped the solvent cage is excluded by the results for **8** with added TEMPO. The lack of 2,3-diphenylbutane formation above 0.02 M TEMPO concentration shows that none of the 2-phenylethyl radicals are available for cross combination. Based on the reduction in yield of **10** on addition of TEMPO, cross combination of cage-free radicals **3** and **14** evidently contributes no more than 5–6% to the total yield of **10** in the absence of TEMPO.

Notably, based on the extent of diffusion and loss of configuration at carbon with **8** and **9**, the radical pairs from these compounds, though evidently relatively long-lived, do not live as long as the triplet pairs formed on direct irradiation (ESR study⁶) of the *p*-acetyl analogue of phosphite **7** (**1**, R = Me, Ar = *p*-MeCOC₆H₄) or on triplet sensitized photolysis (³¹P CIDNP and ESR stud-

ies⁷) of the chiral 1-naphthylmethyl analogue of **6** (**1**, R = Me, Ar = 1-naphthyl). In the triplet-sensitized reaction of **6** itself, about 40% of potentially formed **14** radicals yield dimer **12b**, along with a relatively low yield (20%) of rearranged product, the 1-(1-naphthyl)ethylphosphonate.⁸ Similarly, direct irradiation of **7** itself yields only 20% of the rearrangement product, the 2-(*p*-acetyl)ethylphosphonate, again with a 36–42% accountability yield of dimer (**12**, Ar = *p*-MeCOC₆H₄CH₂).⁸ These systems have not been examined with TEMPO present. Both reactions occur with *near-total loss of configuration at carbon*.⁸ These results are directly opposite to the rearrangement yields, largely retentive stereochemistry at stereogenic carbon, and minor amounts of dimer observed on direct irradiation of phosphites **5** and **6** (Table 4).⁸ The photoreactions of **5** and **6**, as noted earlier, likely occur via *singlet* radical pairs.

Before considering the possible origins of the differences in $k_{\text{comb}}/k_{\text{rot}}$, it must be reemphasized that application of eqs 1–4 to the photorearrangements of **5** and **6** likely is valid. However, the modeling approach shows clearly that when diffusion of **[3,14]**^S and reversible rotation of **14** occur, as must be true for **8** and **9**, the apparent or measured values of R_{obsd} , y (eqs 2 and 3), $k_{\text{comb}}/k_{\text{rot}}$ (eq 4), and percent net retention (eq 5) of Table 4 are *larger* than the actual ones. Consequently, y , $k_{\text{comb}}/k_{\text{rot}}$, and percent net retention for **8** and **9** are *maximum values*. The effects of changing substituents on phosphorus from alkoxy to amino are in fact *larger* than what is indicated by the parameters of Table 4 taken at face value.

Possible Origins of Substituent Effects on the Degree of Retention of Configuration at Carbon and $k_{\text{comb}}/k_{\text{rot}}$. *First*, one could attempt to account for the decrease in $k_{\text{comb}}/k_{\text{rot}}$ with **8** and **9** by an *increase* in k_{rot} . However, it seems intuitively obvious that the amino groups of the pair **[3, 14]** must be sterically larger than MeO and would decrease k_{rot} for radical **14** of the pair **[3,14]**. Furthermore, an increase in k_{rot} cannot account for the sizable *increase* seen in the products of radical diffusion from the solvent cage for **8** and **9** (Table 4).

A *second approach* is to assume that k_{rot} for the pairs **[3,14]** from **5** and **8** is *essentially the same*, and k_{comb} is somehow *decreased* for **14** from **8** and **9**. Thus, with the numbers of Table 4 taken at face value, k_{comb} for the radical pair from **8** is about 6-fold slower than it is for the pair generated by **5** ($[k_{\text{comb}}/k_{\text{rot}}(\mathbf{5})/k_{\text{comb}}/k_{\text{rot}}(\mathbf{8})] = k_{\text{comb}}(\mathbf{5})/k_{\text{comb}}(\mathbf{8}) = 13/2.3 = 5.7$ (both cases with TEMPO present). From the data of Table 4, the value of $k_{\text{comb}}(\mathbf{6})/k_{\text{comb}}(\mathbf{8})$ also must be quite high; however, experiments for **6** with TEMPO present were not done in which case the ratio would be reduced.

As shown in the model approach, neglect of the reversibility of the conversion of *pro-R* **14** to *pro-S* **14** in the use of eqs 1–4 leads to an *increased* apparent or measured value of y . For example, if the *actual* value of y for **8** with added TEMPO is 0.6 (i.e., R_{obsd} , 60) instead of the apparent or measured 0.70 of Table 4, $k_{\text{comb}}/k_{\text{rot}}$ becomes 1.5 instead of 2.3. This reduction would *increase* the value of $k_{\text{comb}}(\mathbf{5})/k_{\text{comb}}(\mathbf{8})$ from 5.7 to 13/1.5 or 8.7. Therefore the estimate for $k_{\text{comb}}(\mathbf{5})/k_{\text{comb}}(\mathbf{8})$ of 5.7, based in Table 4, is a *minimum* value. Evidently, the large *apparent* value of approximately six for $k_{\text{comb}}(\mathbf{5})/k_{\text{comb}}(\mathbf{8})$ is not an artifact of neglect of diffusion of the pair **[3,14]**

or of the reversibility of the conversion of *pro-R* **14** to *pro-S* **14**. The decrease in the value for k_{comb} for **[3,14]** from **8** (and presumably **9**), compared to the corresponding radical pair from **5** (and presumably **6**), must be an inherent property of the reaction system.

Interestingly, the results for the model system for Scheme 1 (which is only an approximation) with reversible rotation of *pro-R* **14**, 20% radical diffusion, and actual $k_{\text{comb}}/k_{\text{rot}} = 1.5$ are similar to those for photorearrangement of **8**. The predicted measured value for $k_{\text{comb}}/k_{\text{rot}}$ is 3.0 (R_{obsd} , 75) compared to the actual value of 1.5 (R_{obsd} , 60).

The large apparent decrease in k_{comb} could be at least in part a result of the differences in *s*-character of the SOMO of **14**, X₂P(O)•. This effect has been seen in the influence of substituents X and Y on the rate constants for addition of XYP(O)• to oxygen and *n*-butylacrylate and for the abstraction of bromine from BrCCl₃ and hydrogen from PhSH.^{15,16} Rates of reaction were increased by increased hyperfine splittings to phosphorus (five radicals, a_P 255–369 G) and consequent increase in *s* character in the SOMO. The range of rate constants at 23 K was 1.7-fold for addition to oxygen; 7-fold for addition to *n*-butyl acrylate; 13-fold for abstraction of hydrogen from PhSH; and 9-fold for abstraction of bromine from BrCCl₃. The phosphorus hyperfine splitting for (MeO)₂P(O)• (a_P , 697 G at 251 °K) is larger than that for (Me₂N)₂P(O)• (a_P , 524 G at 276 °K).¹⁷ Based on the greater *s*-character of its SOMO, (MeO)₂P(O)• from **6** should recombine with **14** more rapidly within the solvent cage than (Me₂N)₂P(O)• from **8**. As a result, the pair [(MeO)₂P(O)•]/**3** would exhibit less diffusion from the solvent cage and greater retention of configuration at the stereogenic carbon of **14**.

However, since the rate constant (k_{comb}) for coupling of **[3,14]** will be very large, its perturbation by change of substituents on **14** from alkoxy to amino may not be great enough to account entirely for the change in k_{comb} . Steric factors also may be associated with the increased diffusion (decreased k_{comb}) of the amino-substituted radicals which will be less pyramidal (smaller a_P) and also feature comparatively bulky amino substituents on phosphorus. Large steric effects on the combination rates of carbon radicals are well-known.¹⁸ The difference in steric size between (Me₂N)₂P(O)• and (MeO)₂P(O)•, along with recombination rate constant differences based on variation in the *s*-character of the SOMO of the two radicals may account for the apparently larger value of k_{comb} for (MeO)₂P(O)•.

Third, a reaction component composed of long-lived *triplet radical pairs*, generated by one of the pathways shown in Scheme 1, could be responsible in part for the configuration loss and enhanced diffusion of radicals formed on photolysis of **8** and **9**. As noted earlier, based on the extent of diffusion and loss of configuration at carbon with **8** and **9**, the radical pairs from these compounds *on average* do not live as long as the distinctly

(15) Sluggett, G. W.; McGarry, P. F.; Koptuyg, I. V.; Turro, N. J. *J. Am. Chem. Soc.* **1996**, *118*, 7367–7372.

(16) Jockusch, S.; Turro, N. J. *J. Am. Chem. Soc.* **1998**, *120*, 11773–11777.

(17) Roberts, B. P.; Singh, K. *J. Organomet. Chem.* **1978**, *159*, 31–35.

(18) Leffler, J. E. *An Introduction to Free Radicals*; John Wiley & Sons: New York, 1993.

triplet pairs formed on direct irradiation of phosphite **7** or from triplet sensitized photolysis of the *l*-naphthylmethyl analogue of **6** reported previously. However, as illustrated in Scheme 1, a fraction of a singlet species, either electronically excited starting material, **13**, or radical pair [**3,14**]^S might undergo intersystem crossing to the corresponding triplet.^{19,20} These possibilities cannot be evaluated at this time.

Further Studies. The presence of triplet radical pairs [**3,14**] from the direct irradiation of the achiral *p*-acetylbenzyl analogue of **7** (**1**, Ar = *p*-acetylphenyl) and triplet sensitized photoreactions of the achiral 1-naphthyl analogue of **6** (**1**, Ar = 1-naphthyl) was demonstrated by ESR-based CIDEP techniques.⁷ ³¹P CIDNP measurements were used to define the presence of triplet [**3,14**] from the analogue of **7** (**1**, Ar = *p*-acetylphenyl).⁶ It is clear that the major pathway for photoreactions of **8** and **9** described in the present paper does not involve triplet [**3,14**]. Nonetheless, further studies of the photoreactions of **8** and **9** will be carried out using triplet quenchers as well as ³¹P CIDNP and time-resolved ESR methods. These magnetic resonance techniques offer the possibility of differentiating the singlet or triplet spin characteristics of radical pairs involved in the photochemistry from the phase of spin polarization observed. The presence of a triplet component might account for or at least contribute to the loss of stereochemistry and increased extent of radical diffusion encountered with these phosphorodiamidite.

Steric effects on the diffusive separation of the radicals [**3,14**]^S should be amenable to study by use of more sterically bulky amino groups, i.e., *i*-Pr₂N instead of Me₂N.

Conclusions

On irradiation, phosphorodiamidites **8** and **9** undergo the photo-Arbuzov rearrangement reaction to give **10** and **11**, respectively, as major products. Also formed are the products of radical pair diffusion and dimerization, the 2,3-diarylbutanes **12a** and **12b**. Like the previously studied phosphites **5** and **6**, the photoreactions of the phosphorodiamidite are most simply understood as proceeding primarily via singlet radical pairs [**3,14**]^S (Scheme 1). Notably, **8** and **9** give significantly increased amounts of dimer **12** compared to **5** and **6**. Furthermore, the loss of configuration at the stereogenic carbon in products **10** and **11** is considerably increased over what is observed with phosphites **5** and **6**. The radical pairs from **8** and **9** must be relatively long-lived compared to those from **5** and **6**. As measured by eq 5, $k_{\text{comb}}/k_{\text{rot}}$ is reduced for the radical pair [**3,14**] from **8** (TEMPO present) and **9** compared to the same parameters for phosphites **5** (TEMPO present) and **6** (Table 4). Arguments that include use of a simple model system are made to show that the reduced $k_{\text{comb}}/k_{\text{rot}}$ is not the result of the neglect in the application of eqs 1–5 of the reversal of the rotation of radical **14** and of diffusion of the pair [**3,14**]^S. Evidently, the measured $k_{\text{comb}}/k_{\text{rot}}$ of 2.3 is in fact a maximum value. It is proposed that the reduced $k_{\text{comb}}/k_{\text{rot}}$

values for the radicals from **8** and **9** most likely results from a decrease in k_{comb} for the phosphinoyl radicals, (Me₂N)₂P(O)[•], from **8** and **9** which also accounts for increased radical pair diffusion and loss of configuration through rotation of radical **14** within the solvent cage. A ratio of k_{comb} for the two systems is calculated from the data of Table 4, assuming k_{rot} to be the same. A minimum value of 5–6 for $k_{\text{comb}}(\mathbf{5})/k_{\text{comb}}(\mathbf{8})$ in favor of the pair from **6** is estimated. The decrease in k_{comb} may arise at least in part from the known lower degree of *s*-character in the SOMO of diaminophosphinoyl radicals [X₂P(O)[•]; X, = amino], indicated by ESR hyperfine splittings, and consequent reduced reactivity toward the 1-arylethyl radical, **14**, in the solvent cage. Steric factors may also play a part in making the more nearly planar, amino-substituted radicals (decreased SOMO *s*-character) less prone to cage recombination. In addition the apparent reduced $k_{\text{comb}}/k_{\text{rot}}$ and increased radical diffusion observed for **8** and **9** might not be totally a function of singlet pair lifetimes if a triplet radical pair component (Scheme 1) is present. Further insight will be sought in future investigations of **8** and **9** using triplet quenchers as well as ³¹P CIDNP and ESR magnetic resonance techniques.

Photo-Arbuzov rearrangements of phosphites related to **1**–**6** are synthetically useful.^{4,5} However, the synthetic utility of the photorearrangements of phosphodiamidites analogous to **8** and **9** remains to be evaluated.

Experimental Section

Spectroscopic Data. *J* for the ¹H NMR data refer to proton–proton coupling unless otherwise stated. Ultraviolet (UV) spectra were obtained in acetonitrile and cyclohexane on a diode array spectrophotometer. Wavelength maxima (λ_{max}) are reported in nm with extinction coefficients, ϵ , in M⁻¹ cm⁻¹.

Irradiation Experiments. Procedures for the preparation under argon of 0.01 M solutions of **8** and **9** with an appropriate amount of tri-*n*-propyl phosphate for quantitative studies and for the ensuing analyses by GLC of the photoreactions of **8** and **9**, were described earlier for the phosphites **5**–**7**.⁸ Phosphoramidite **8** was irradiated in a Rayonet reactor through quartz at 254 nm while **9** was irradiated with the Rayonet apparatus through Pyrex at 300 nm at the concentrations recorded in Tables 1–3. Quantitative gas chromatographic analyses for **8**–**11** and **12** were done with a flame ionization detector (FID) and a DB-1 (1% methyl silicone) capillary column (10 or 30 m × 0.25 mm × 0.25 mm) with tri-*n*-propyl phosphate as internal standard. LRMS and HRMS were performed in the EI (70 eV) or CI mode as were GC/MS analyses (15 or 30 m × 0.25 mm × 0.25 mm DB-1 capillary column). The techniques recorded below for purification of the enantiomeric phosphoroamidates **10** and **11** and determination of their enantiomeric composition by chiral HPLC are completely analogous to the methods described in detail for the phosphonates from photorearrangement of **5** and **6**.⁸

Determinations of Enantiomeric Compositions of Products. Column chromatography (silica gel, chloroform) prepurification was done on all mixtures (**10**, **11** and oxides of **8** and **9**) to be purified or analyzed by HPLC. The prepurified material was dissolved in 1–2 mL of the intended HPLC eluent, and the solution was filtered through a Millex-HV₁₃ (0.45 μm, 13 mm diameter) filter unit. The commonly used solvent system was 1.3–1.7% methanol in chloroform. Separations and analyses by HPLC were done under isocratic conditions (UV detector) on 4.6 mm i.d. analytical, 10 mm i.d. semipreparative, and 21.4 mm i.d. preparative Dynamax HPLC columns (100 Å spherical Microsorb packings in 5 mm particle size).

(19) Gilbert, A.; Baggott, J. *Essentials of Molecular Photochemistry*; Blackwell Scientific: London, 1991.

(20) Turro, N. J.; Buchachenko, A. L.; Tarasov, V. F. *Acc. Chem. Res.* **1995**, *28*, 69–80.

Chiral HPLC analyses employed a CHIRALCEL OD HPLC column (250 mm × 4.6 mm i.d.), equipped with a 50 mm × 4.6 mm i.d. guard column. Mobile phases used were 95:5–90:10 of hexanes/2-propanol. Optimum flow rate was 1.0 mL/min. Initial (Tables 1–3) and subsequent *R/S* ratios (Supporting Information) for **8** and **9** (Tables 1–3) were determined by chiral HPLC analysis on their oxides formed on oxidation by *tert*-butyl hydroperoxide.^{8,9} The enantiomeric ratios for **10** and **11** recorded in Tables 1–3 as a function of conversion of **8** and **9** were also determined by chiral HPLC analysis following the separation of the oxide and phosphorodiamidate rearrangement product.

Preparation of 1-Phenylethyl *N,N,N,N*-Tetramethylphosphorodiamidite (8). At room temperature under argon atmosphere, a solution of 1-phenylethanol (3.0 g, 25 mol.) in 10 mL of acetonitrile was added dropwise to a solution of hexamethylphosphoruric triamide (4.4 g, 27 mol.) and a catalytic amount of 1-*H*-tetrazole (18 mg, 0.28 mmol) in 20 mL of acetonitrile. The solution was stirred at room temperature for an additional 1 h. The solvent was removed in vacuo. A 15 mL portion of a 1:1 mixture of dry ether and ethyl acetate was added to the residue. The solid was filtered off in a Schlenk apparatus under argon. Solvent removal in vacuo followed by vacuum distillation gave **8** (4.0 g, 17 mmol, 63%) as a colorless liquid: bp 55–56 °C (0.05 mmHg) (99% purity by GC); ³¹P NMR (121 MHz, CDCl₃, {¹H}) δ 140.4; ¹H NMR (300 MHz, CDCl₃) δ 1.18 (d, 6 H, ³J = 6.6 Hz), 2.11 (d, 6 H, ³J_{HP} = 8.8 Hz), 2.27 (d, 3 H, ³J_{HP} = 9.0 Hz), 4.66 (dq, 1 H, ³J_{HP} = 9.4 Hz, ³J = 6.5 Hz), 6.77–7.07 (m, 5 H); ¹³C NMR (75 MHz, CDCl₃, {¹H}) δ 25.0 (d, ²J_{CP} = 5.8 Hz), 36.5 (d, ²J_{CP} = 18.2 Hz), 36.8 (d, ²J_{CP} = 17.9 Hz), 72.7 (d, ²J_{CP} = 19.8 Hz), 125.8, 127.0, 128.1, 145.0 (d, ³J_{CP} = 3.2 Hz); UV (CH₃CN) 258 (ε 866); GC–EIMS (70 eV) *m/z* (relative intensity) 240 [M]⁺ (12), 226 (12), 135 (100), 105(10). Anal. Calcd for C₁₂H₂₁N₂OP: C, 59.98; H, 8.81; N, 11.66. Found: C, 60.09; H, 8.88; N, 11.65.

(*R*)-1-Phenylethyl *N,N,N,N*-Tetramethylphosphorodiamidite (8**).** By the procedure used for the preparation of racemic **8**, reaction of hexamethylphosphoruric triamide (1.1 g, 6.7 mmol), 0.80 g (6.5 mmol) of (*R*)-1-phenylethanol (99:1 *R/S*), and 1-*H*-tetrazole (4.3 mg, 0.6 mmol) followed by distillation gave 0.99 g (4.1 mmol, 62%) of (*R*)-**8**; 99% purity by GC, 99:1 *R/S* ratio determined on the corresponding oxide from oxidation by *tert*-butyl hydroperoxide.^{8,9}

1-Phenylethyl *N,N,N,N*-Tetramethylphosphonic Acid Diamide (10). On irradiation at 254 nm approximately 0.3 g of phosphorodiamidite **8** in benzene was partially converted to **10** which was isolated from the product mixture in 99% GC purity by HPLC (1.5% methanol in chloroform): ³¹P NMR (121 MHz, CDCl₃, {¹H}) δ 37.5; ¹H NMR (300 MHz, CDCl₃) δ 1.55 (dd, 3 H, ³J_{HP} = 16.4 Hz, ³J = 7.3 Hz), 2.31 (d, 6 H, ³J_{HP} = 9.0 Hz), 2.7 (d, 6 H, ³J_{HP} = 8.6 Hz), 3.30 (dq, 1 H, ²J_{HP} = 14.3 Hz, ³J = 7.2 Hz), 7.20–7.43 (m, 5 H); ¹³C NMR (75 MHz, CDCl₃, {¹H}) δ 17.1 (d, ²J_{CP} = 4.2 Hz), 36.3 (d, ²J_{CP} = 3.1 Hz), 36.6 (d, ²J_{CP} = 3.1 Hz), 75.1 (d, ¹J_{CP} = 109.5 Hz), 126.6 (d, *J*_{CP} = 2.6 Hz), 128.3 (d, *J*_{CP} = 2.1 Hz), 128.8 (d, *J*_{CP} = 6.2 Hz), 139.9 (d, ²J_{CP} = 5.7 Hz); UV (CH₃CN): 248 (ε 123), 254 (ε 165), 260 (ε 194), 266 (ε 143); GC–EIMS (70 eV) *m/z* (relative intensity) 240 [M]⁺, 226, 135 (100), 105(6). Anal. Calcd for C₁₂H₂₁N₂OP: C, 59.98; H, 8.81; N, 11.66. Found: C, 59.96; H, 8.83; N, 11.73.

2-(1-(1-Naphthyl)ethoxy)-1,3-dimethyl-1,3,2-diazaphospholane (9) was prepared by the reaction of 2-diethylamino-1,3-dimethyl-1,3,2-diazaphospholane (1.2 g, 0.059 mmol) and 1-(1-naphthyl) ethanol (1.1 g, 0.064 mmol) following the procedure for preparation of phosphoramidite **8**. Flash chromatography gave **9** as a colorless thick oil (1.2 g, 0.042 mmol, 71%): ³¹P NMR (121 MHz, CDCl₃, {¹H}) δ 128.9; ¹H NMR (300 MHz, CDCl₃) δ 1.60 (d, 3 H, ³J = 6.4 Hz), 2.46 (d, 3 H, ³J_{HP} = 12.5 Hz), 2.47 (d, 3 H, ³J_{HP} = 12.5 Hz), 2.88–3.29 (m, 4 H),

5.72 (dq, 1 H, ³J_{HP} = 8.6 Hz, ³J = 6.6 Hz), 7.39–7.50 (m, 3 H), 7.63–7.83 (m, 3 H), 8.13 (d, 1 H, *J* = 8.3); ¹³C NMR (75 MHz, CDCl₃, {¹H}) δ 25.4 (d, ²J_{CP} = 3.1 Hz), 33.88 (d, ²J_{CP} = 23.4 Hz), 33.93 (d, ²J_{CP} = 23.9 Hz), 52.6 (d, ²J_{CP} = 9.9 Hz), 52.8 (d, ²J_{CP} = 9.9 Hz), 68.4 (d, ²J_{CP} = 11.4 Hz), 123.1, 123.2, 125.1, 125.33, 125.5, 127.2, 128.7, 129.9, 133.4, 141.3, (d, *J*_{CP} = 1.6 Hz); UV (CH₃CN): 262 (ε 5.3 × 10³), 272 (ε 7.9 × 10³), 282 (ε 9.3 × 10³), 294 (ε 6.7 × 10³); GC–EIMS (70 eV) *m/z* (relative intensity) 288 [M]⁺ (5), 155 (26), 133 (100), 127 (9); HRMS [M]⁺ calcd for C₁₆H₂₁N₂OP 288.1392, found 288.1392. By the same procedure, (**R**)-2-(1-(1-Naphthyl)ethoxy)-1,3-dimethyl-1,3,2-diazaphospholane (**9**) (*R/S* = 98:2) was prepared in sufficient quantities for the stereochemical studies.

2-(1-(1-Naphthyl)ethoxy)-2-oxo-1,3-dimethyl-1,3,2-diazaphospholane (10-O) was isolated from oxidation of a 0.3–0.5 g sample of **9** with 3 M *tert*-butyl hydroperoxide⁹ by the procedure established previously for phosphites followed by HPLC purification of a portion of the product (1.1% methanol in chloroform): ³¹P NMR (121 MHz, CDCl₃, {¹H}) δ 0.84; ¹H NMR (300 MHz, CDCl₃) δ 1.74 (d, 3 H, ³J = 6.4 Hz), 2.36 (d, 6 H, ³J_{HP} = 9.8 Hz), 2.98–3.15 (m, 4 H), 6.03 (dq, 1 H, ³J_{HP} = 9.7 Hz, ³J = 6.7 Hz), 7.45–7.56 (m, 3 H), 7.69 (d, 1 H, *J* = 6.6 Hz), 7.78 (d, 1 H, *J* = 8.3 Hz), 7.85–7.88 (m, 1 H), 8.15–8.18 (m, 1 H); ¹³C NMR (75 MHz, CDCl₃, {¹H}) δ 24.5 (d, ³J_{CP} = 5.7 Hz), 31.5 (d, ²J_{CP} = 4.2 Hz), 31.7 (d, ²J_{CP} = 4.2 Hz), 46.7 (d, ²J_{CP} = 14.5 Hz), 46.9 (d, ²J_{CP} = 13.5 Hz), 72.6 (d, ²J_{CP} = 7.3 Hz), 123.2, 123.3, 125.3, 125.5, 126.0, 128.1, 128.8, 129.79, 133.7, 138.9 (d, *J*_{CP} = 3.6 Hz); GC–EIMS (70 eV) *m/z* (relative intensity) 304 [M]⁺ (24), 155 (39), 154 (100), 127 (11); HRMS [M]⁺ calcd for C₁₆H₂₁N₂O₂P 304.1341, found 304.1355.

1-Phenylethyl *N,N,N,N*-tetramethylphosphorodiamidite oxide (8-O) was formed by the same procedure^{8,9} used to obtain **10-O** and isolated by HPLC purification. The thick oil was shown to be >99% pure by GC analysis.

2-(1-(1-Naphthyl)ethyl)-2-oxo-1,3-dimethyl-1,3,2-diazaphospholane (11) was isolated in 99% GC purity by HPLC (1% methanol in chloroform) from the mixture obtained by irradiation to partial conversion of diazaphospholane **9** at 300 nm in benzene on an approximately 0.5 g scale: ³¹P NMR (121 MHz, CDCl₃, {¹H}) δ 129.3; ¹H NMR (300 MHz, CDCl₃) δ 1.73 (dd, 3 H, ³J_{HP} = 17.0 Hz, ³J = 7.2 Hz), 2.43 (d, 3 H, ³J_{HP} = 9.0 Hz), 2.46 (d, 3 H, ³J_{HP} = 8.8 Hz), 2.77–3.03 (m, 4 H), 4.20 (dq, 1 H, ²J_{HP} = 19.3 Hz, ³J = 7.3 Hz), 7.43–7.55 (m, 3 H), 7.60–7.64 (m, 1 H), 7.71–7.74 (m, 1 H), 7.82–7.85 (m, 1 H), 8.14 (d, 1 H, *J* = 8.3 Hz); ¹³C NMR (75 MHz, CDCl₃, {¹H}) δ 17.0 (d, ³J_{CP} = 4.2 Hz), 32.5 (d, ²J_{CP} = 4.9 Hz), 32.6 (d, ²J_{CP} = 5.2 Hz), 34.8 (d, ¹J_{CP} = 117.8 Hz), 47.4 (d, ²J_{CP} = 8.3 Hz), 47.6 (d, ²J_{CP} = 8.3 Hz), 123.0, 124.9, 125.0, 125.1 (d, *J*_{CP} = 18.2 Hz), 125.6, 126.8 (d, *J*_{CP} = 3.6 Hz), 128.7, 131.4 (d, *J*_{CP} = 5.7 Hz), 133.6 (d, *J*_{CP} = 2.1 Hz), 136.0 (d, *J*_{CP} = 6.2); UV (CH₃CN): 266 (ε 4.7 × 10⁴), 276 (ε 7.4 × 10⁴), 286 (ε 8.9 × 10⁴), 298 (ε 6.1 × 10⁴); GC–EIMS (70 eV) *m/z* (relative intensity) 288 [M]⁺ (14), 155 (10), 133 (100). Anal. Calcd for C₁₆H₂₁N₂OP: C, 66.65; H, 7.34; N, 9.72. Found: C, 66.66; H, 7.31; N, 9.70.

Acknowledgment. This research was supported by grants from the National Science Foundation and the National Institutes of Health.

Supporting Information Available: General experimental information; preparations and spectral data for the precursors to phosphorodiamidite **9**; tables showing the configurational stabilities of unreacted **8** and **9** over the course of irradiation. This material is available free of charge via the Internet at <http://pubs.acs.org>.

JO040297+